[1]Department of Neurosurgery,
University of Marburg
Chairman: Prof. Dr. med. Ch. Nimsky
[2]Computer Graphics Group,
University of Siegen
Chairman: Prof. Dr. A. Kolb
[3]Department of Mathematics and Computer Science,
University of Marburg
Distributed Systems Group
Chairman: Prof. Dr. B. Freisleben

6th Russian-Bavarian Conference on
Bio-Medical Engineering (RBC)
November 8-12, 2010, Moscow, Russia

A Comparison of Two Human Brain Tumor Segmentation Methods

Egger J[1,3], Zukic Dž[2], Bauer M H A[1,3], Kuhnt D[1], Carl B[1], Freisleben B[3], Kolb A[2], Nimsky Ch[1]

Introduction:

The most common primary brain tumors are gliomas, whereof 70% are among the group of malignant gliomas (anaplastic astrocytoma World Health Organization (WHO) grade III, glioblastoma multiforme (GBM) WHO grade IV). The GBM is one of the highest malignant human neoplasms. Due to the biological behavior, gliomas of WHO grade II to IV cannot be cured with surgery alone. The multimodal therapeutical concept involves maximum safe resection followed by radiation and chemotherapy, depending on the patient's Karnofsky scale. The survival rate is still only approximately 15 months, despite new technical and medical accomplishments such as multimodal navigation during microsurgery, stereotactic radiation or the implementation of alkylating substances.

Materials and Methods:

For the segmentation process of the pathologies (GBM WHO grade IV), we used 1.5 Tesla magnetic resonance imaging (MRI) scans from the clinical routine. For the glioblastomas, we chose T1-weighted images after gadolinium-enhancement (mostly axial).

Balloon inflation forces: The main idea is to start with a small triangular surface mesh in the shape of a convex polyhedron at the approximate center of the glioma. Balloon inflation forces are then used to expand this mesh iteratively, each iteration step consisting of:

- Splitting of long edges (mesh refinement)
- Computation of surface normals and estimation of curvature (per vertex)
- Inflation (moving vertices outwards)
- Slight smoothing of the mesh

Graph-based approach: The overall graph-based method starts by setting up a directed 3D graph from a user-defined seed point that is located inside the object. To set up the graph, the method samples along rays that are sent through the surface points of a polyhedron with the seed point as center. The sampled points are the nodes $n \in V$ of the graph G(V,E) and E is a corresponding set of edges $e \in E$.

After graph construction, the minimal cost closed set on the graph is computed via a polynomial time s-t cut. The s-t cut creates an optimal segmentation of the object under the influence of the parameter Δ_r that controls the stiffness of the surface. A delta value Δ_r of 0 would ensure that the segmentation result is a sphere.

Results:

The presented method using balloon inflation forces has been implemented in C++. The segmentation took about 1 second per data set on an Intel Core i7-920 CPU, 2.66 GHz (4 cores), on Windows7 x64. The graph-based approach has been implemented in C++ within the MeVisLab platform. Using 2432 and 7292 polyhedra surface points, the overall segmentation (sending rays, graph construction and min-cut computation) took less than 5 seconds on an Intel Core i5-750 CPU, 4x2.66 GHz, 8 GB RAM, Windows XP Professional x64 Version, Version 2003, SP 2. Manual segmentation took 6.93±4.11 minutes (minimum 3 minutes and maximum 19 minutes).

	Volume of tumor (cm^3)			Number of voxels			$DSC_{balloon}$ (%)	DSC_{graph} (%)
	manual	balloon	graph	manual	balloon	graph		
min	3.78	1.90	5.03	18773	9445	21598	65.71	76.82
max	73.45	46.56	65.60	253512	158371	252316	89.50	93.82
$\mu \pm \sigma$	31.00 ± 23.80	23.08 ± 16.25	26.48 ± 21.01	88404.29	65852.00	83653.14	78.27 ± 7.69	86.11 ± 7.38

Table 1: Summary of results: min., max., mean and standard deviation for both approaches

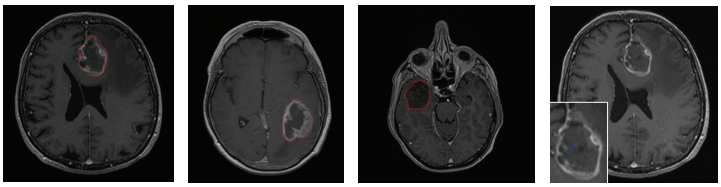

Figure 1: Initialization for balloon inflation forces approach and graph-based approach (rightmost)

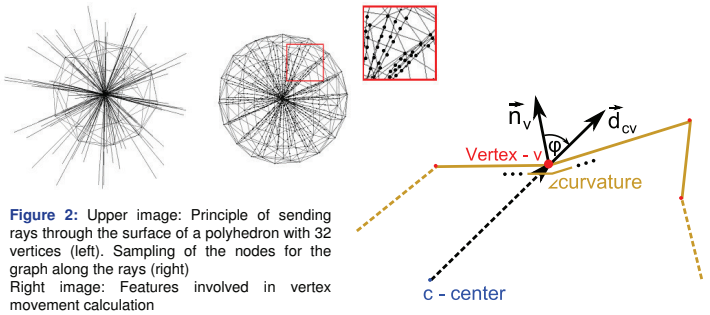

Figure 2: Upper image: Principle of sending rays through the surface of a polyhedron with 32 vertices (left). Sampling of the nodes for the graph along the rays (right)
Right image: Features involved in vertex movement calculation

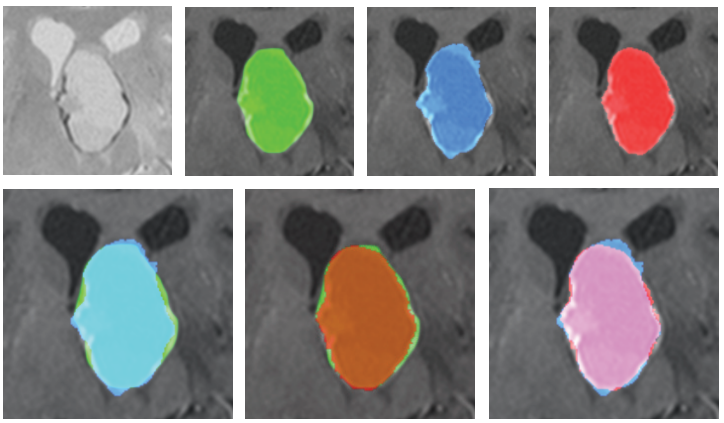

Figure 3: First row: Close-up of one slice of the original image (left). Segmented tumor: manual (green), balloon inflation forces (blue) and graph-based (red). Second row – overlaps: cyan = manual + inflation forces, brown = manual + graph-based, pink = inflation forces + graph-based

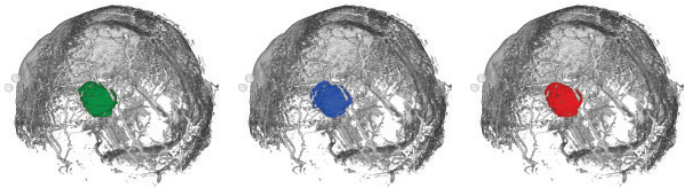

Figure 4: Segmented tumor: manual segmentation (left), segmentation with balloon inflation forces (middle) and graph-based segmentation (right)

Conclusion:

In this contribution, two approaches for WHO grade IV glioma segmentation have been presented, evaluated and compared against each other. One method uses balloon inflation forces and relies on the detection of high-intensity tumor boundaries that are coupled with the use of contrast agent gadolinium. The other method sets up a directed and weighted graph and performs a min-cut for optimal segmentation results. The presented approaches have been compared and evaluated on various MRI datasets with WHO grade IV gliomas. Experts (neurosurgeons) with several years of experience in the resection of gliomas extracted the tumor boundaries manually to obtain the ground truth for the given data. The manually segmented results and the segmentation results of the presented approaches have been compared by calculating the average Dice Similarity Coefficient.

References:

1. Kleihues, P., Louis, D. N., Scheithauer, B. W., Rorke, L. B., Reifenberger, G., Burger, P. C., Cavenee, W. K.: The WHO classification of tumors of the nervous system. Journal of Neuropathology & Experimental Neurology; 61(3): 215-229 (2002)
2. Egger, J., Bauer, M. H. A., Kuhnt, D., Carl, B., Kappus, C., Freisleben, B., Nimsky, Ch.: Nugget-Cut: A Segmentation Scheme for Spherically- and Elliptically-Shaped 3D Objects. DAGM, LNCS 6376, pp. 383–392, Springer, Darmstadt, Germany (2010)
3. Cohen, L. D.: On active contour models and balloons, Computer Vision, Graphics, and Image Processing (CVGIP): Image Understanding, Volume 53(2), 211-218 (1991)
4. Boykov, Y., Kolmogorov, V.: An Experimental Comparison of Min-Cut/Max-Flow Algorithms for Energy Minimization in Vision. IEEE Transactions on Pattern Analysis and Machine Intelligence, 26(9), pp. 1124-1137 (2004)
5. MeVisLab – development environment for medical image processing and visualization. MeVis Medical Solutions AG and Fraunhofer MEVIS, Bremen, Germany. http://www.mevislab.de
6. Zou, K. H., Warfield, S. K., Bharatha, A., et al.: Statistical Validation of Image Segmentation Quality Based on a Spatial Overlap Index: Scientific Reports. Academic Radiology, 11(2), pp. 178-189 (2004)

Correspondence:
Dr. J. Egger, Department of Neurosurgery, University of Marburg
Baldingerstrasse, 35033 Marburg, Germany
egger@med.uni-marburg.de, www.neurochirurgie-marburg.de